



Essential Oil Composition, Cytotoxicity against Hepatocellular Carcinoma, and Macro and Micro-Morphological Fingerprint of *Laurus nobilis* Cultivated in Egypt

Nesma Nagah, Islam Mostafa[#], Gamal Dora, Zeinab El-Sayed, Abdel-Monem Ateya
 Department of Pharmacognosy, Faculty of Pharmacy, Zagazig University, Zagazig,
 44519, Egypt.



CrossMark

GC/MS analysis of hydro-distilled essential oil (1.9% v/w) from fresh leaves of *Laurus nobilis* cultivated in Egypt revealed the presence of 81 components from which 59 compounds were identified, the identified compounds represent 96.3 % of the oil composition. The major constituents were 1,8-cineole (27.41%), linalool (19.37%), α -terpinyl acetate (14.65%), methyl eugenol (7.73%), α -terpineol, (2.84%), terpinen-4-ol (2.09%), elemicin (2.08%) and sabinene (1.80%). Qualitative and quantitative identification of the essential oil constituents was based on comparison of retention indices (RIs) of standard n-alkanes (C_8 - C_{24}) and mass spectra of the oil components with those reported in the literature. The essential oil exhibited potent cytotoxic activity against *Hep-G2* (IC_{50} = 1.83 μ g/mL). The cytotoxic activity study was enriched using molecular docking analysis of the oil components against caspase3 (apoptotic enzyme). The docking reflected the ability of 32 compounds to interact with caspase3 at different sites and initiating its activity. Moreover, macro- and micromorphological studies of the plant's leaves, petioles and stem in both entire and isolated elements forms were carried out. They reflected the presence of characteristic oil cells and fibers in the leaves, petioles and stems in addition to mucilage cells in the leaves and petioles, sclereids in the leaves and old stems and small trichomes on the young stem surface.

Keywords: Cytotoxicity, Essential oil, GC/MS, *Hep-G2*, *Laurus nobilis*, Macro- and micromorphology, Molecular docking.

Introduction

Laurus nobilis Linn. also known as sweet bay leaf, true bay and bay laurel is a small aromatic evergreen tree of Lauraceae family which grows up to 20 m in height with green simple leaves, smooth bark, yellowish white flowers and small purple olive-like fruits (Charles, 2013). The plant is native to the Mediterranean region and Asia, it is cultivated in Algeria, Morocco, Italy, Portugal, Spain and Russia (Serebrynaya et al., 2017). The tree is grown as decorative species throughout Europe and America (Fidan et al., 2019). Chemical composition of *L. nobilis* is characterized by essential oil, sesquiterpenoids, flavonoids and other compounds (El-Sawi et al., 2009; Patrakar et al., 2012; Nagah et al., 2021). *Laurus* extracts

and essential oil have exerted many biological activities such as: antimicrobial (Saleh et al., 2019), analgesic and anti-inflammatory (Lee et al., 2019) and cytotoxic activity against different cell lines (Moteki et al., 2002; Abu-Dahab et al., 2014; Saab et al., 2015; Saeed et al., 2016). Previous studies reflected variation in the essential oil components and their percentage from *L. nobilis* growing in different regions (Yalçın et al., 2007; El-Sawi et al., 2009; Fidan et al., 2019; Nafis et al., 2020; Tomar et al., 2020). In this study, we aimed to figure out essential oil components of *L. nobilis* leaves cultivated in Egypt as well as testing its cytotoxic activity against *Hep-G2* cells and finding out the oil components which are responsible for the activity using molecular docking. Moreover, for the first time, detailed morphological and histological

[#]Corresponding author email: islam_mostafa_elbaz@yahoo.com

Tel/Fax: +20552303266

Received 3/1/ 2021; Accepted 17/3/ 2021

DOI: 10.21608/ejbo.2021.56342.1603

Edited by: Prof. Dr.: Abdelfattah Badr, Faculty of Science, Helwan University, Cairo, Egypt.

©2021 National Information and Documentation Center (NIDOC)

examinations of the leaf and stem were carried out to assist the Egyptian plant identification.

Materials and Method

Plant material

The cultivated fresh plant materials were collected from trees growing in El-Orman Botanical Garden, Giza, Egypt in July 2020. The plant was kindly identified by Mrs. Traes Labib, general manager and head of specialists for plant taxonomy in El-Orman Botanical Garden, Giza, Egypt. A Voucher specimen was kept in Pharmacognosy Department, Faculty of Pharmacy, Zagazig University, Egypt.

Essential oil preparation and GC/MS analysis

About 100g of fresh leaves were hydro-distilled for 4hrs. using Clevenger apparatus. The resulted oil was dried over anhydrous sodium sulfate and stored at 4°C in amber glass vial until analysis. Qualitative and quantitative GC/MS analysis was performed using Shimadzu GC/MS-QP2010 (Koyoto, Japan) equipped with Rtx®-5MS fused bonded column (30m x 0.25mm i.d. x 0.25µm film thickness) (Restek, USA) which is equivalent to DB5. The initial column temperature was kept at 45°C for 2min. (isothermal) and programmed to 300°C at a rate of 5°C/min. and kept constant at 300°C for 5min. (isothermal), injector temperature was 250°C. Helium carrier gas flow rate was 1.41mL/min. All the mass spectra were recorded applying the following condition: (equipment current) filament emission current, 60mA; ionization voltage, 70eV; ion source, 200°C. Diluted sample (1% v/v) was injected with split mode (split ratio 1: 15). Retention indices (RI) were calculated with respect to a set of co-injected standard *n*- alkanes (C₈-C₂₄) and were analyzed separately by GC/MS under the same chromatographic conditions using the same Rtx®-5MS column.

Cytotoxic activity

Regarding cytotoxicity assay, *L. nobilis* oil was assessed using cell viability assay as described by Mosmann (1983), Gomha et al. (2015). Briefly, the cells of HepG-2 were seeded in 96-well plate at a cell concentration of 1×10⁴ cells per well in 100µL of growth medium (Dulbecco's modified Eagle's medium (DMEM) supplemented with 10% heat-inactivated fetal bovine serum, 1% L-glutamine, HEPES buffer and 50µg/mL gentamycin). After 24hrs. of seeding, fresh media containing different

concentrations of the tested samples (Two-fold serial dilutions) were dispensed into the 96-well and incubated at 37°C in a humidified incubator with 5% CO₂ for a period of 48hrs. Three wells were used for each concentration of the tested samples. Control cells were incubated without any tested samples and with or without DMSO. The little percentage of DMSO present in the wells (maximal 0.1%) was not found to affect the experiment. The incubation was continued for 24hrs. and after that, media were aspirated and crystal violet solution (1%) was added to each well for at least 30min. The excess stain was removed and glacial acetic acid (30%) was then added to the wells, mixed thoroughly, and then the optical density (OD) was measured with the microplate reader (SunRise, TECAN, Inc, USA) to determine the number of viable cells. The percentage of viability was calculated by comparing the treated samples with the control cells. All experiments were carried out in triplicates. The cell cytotoxic effect of tested oil was calculated. The relation between surviving cells and oil concentration was plotted to show the survival curve of tumor cell line after treatment with the oil. The 50% inhibitory concentration (IC₅₀) was estimated from graphic plots of the dose response curve for each oil concentration using Graphpad Prism software (San Diego, CA. USA). Vinblastine sulfate was used as standard (IC₅₀= 2.93µg/mL).

Molecular docking study

Molecular docking of *L. nobilis* essential oil components' was carried out using Molecular Operating Environment 2009 (MOE) as previously described by Nagah et al. (2021). Briefly, the compounds were constructed in 3D structure, their energies were minimized and saved to MDB file. Caspase3 (responsible for *Hep-G2* apoptosis) X-ray crystallographic structure coded as 2J30 was downloaded from the Protein Data Bank (R.P.D. Bank, RCSB PDB: Homepage, 2020. <https://www.rcsb.org/> (accessed 2 December 2020). Hydrogen atoms were added to the protein structure and missed connections and their types were corrected automatically. The receptor and its atoms potential were fixed. The active site of the enzyme was determined based on co-downloaded natural ligand and using surfaces and maps.

The constructed compounds' database was docked against caspase3 using triangle matcher for placement; London dG with ten retains for scores and force field for refinement. Energy, root-mean

square deviation (rmsd) and formed interactions (bonds) were examined to select between the resulted poses.

Macro- and micromorphological studies

For the macro- and micromorphological studies, samples of leaf, petiole, young and old stem were preserved in a mixture of ethyl alcohol: glycerin: water (1:1:1, v/v) and stored in a tightly closed container. Transverse sections in leaf base, petiole, young and old stem were stained with safranin and fast green dye.

Results and Discussion

GC/MS analysis of the essential oil of the leaves of *Laurus nobilis*

Hydro-distillation of fresh leaves of *Laurus nobilis* afforded 1.9% v/w pale yellow oil with pleasant aromatic odour, moisture free oil. GC/MS analysis of the essential oil (Fig. 1) revealed the presence of 81 components from which 59 compounds were identified. The identified compounds represent 96.3 % of the oil composition. Identification of the oil constituents was based on comparison of the retention indices (RIs) and mass spectra of the oil components with those reported in the previous literatures (Adams, 1995; Ozcan et al., 2010; Abu-Dahab et al., 2014; Taoudiat et al., 2018; Fidan et al., 2019; Tomar et al., 2020). This is the first time for identification of essential oil components of *L. nobilis* cultivated in Egypt based on Retention indexes. The identified compounds are listed in order of their elution from Rtx®-5MS

capillary column with their RT, RI and relative percentages (Table 1).

The essential oil of the fresh leaves was found to be rich with oxygenated monoterpenes representing 69.19% and including 1,8-cineole (27.41%) as the major compound, followed by linalool (19.37%) and α -terpinyl acetate (14.65%). Also, amounts of α -terpineol (2.84%) and terpinen-4-ol (2.09%) were detected. Aromatic compounds showed the next major class (11.92%) with methyl eugenol (7.73%) as the major aromatic followed by elimicin (2.08%), eugenol (1.56%) and cinnamyl acetate (0.55%). Monoterpene hydrocarbons reported significant contribution in *L. nobilis* essential oil composition by about 5.81%. The major monoterpene hydrocarbons are sabinene (1.80%), γ -terpinene (0.72%), α -pinene (0.67%), β -myrcene (0.54%), β -pinene (0.38%), 3-carene (0.38%) and terpinolene (0.34%). Oxygenated sesquiterpenes is another important class (5.64%) with the following constituents: α -cadinol (1.42%), shyobunol (0.99%), spathulenol (0.81%), τ -muurolol (0.63%), viridiflorol (0.43%), 1-epi-cubenol (0.26%), cubebol (0.22%), α -muurolol (0.17%), elemol (0.15%) and eudesma-4(15),7-dien-1- β -ol (0.15%). As to sesquiterpene hydrocarbons, B-elemene (0.98%), bicyclogermacrene (0.94%), δ -cadinene (0.58%), germacrene D (0.29%), alloaromadendrene (0.21%), α -humulene (0.18%), α -copaene (0.17%), γ -muurolene (0.17%), β -caryophyllene (0.16%) and β -selinene (0.15%) were the major components summing up to 4.27%. Other components were detected in lower amounts.

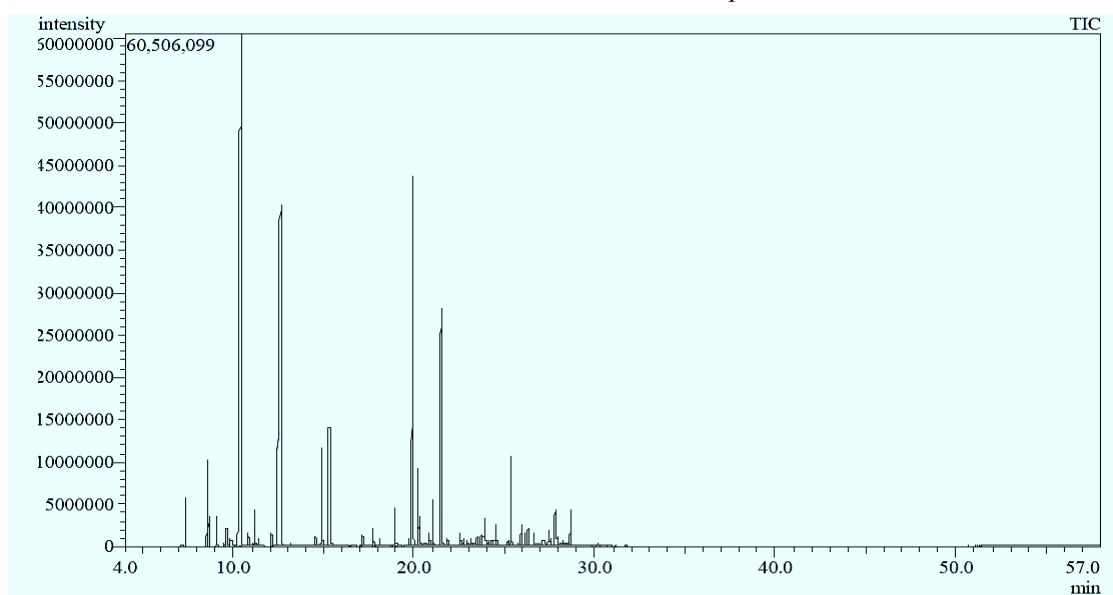


Fig. 1. GC/MS chromatogram of essential oil from *L. nobilis* leaves

TABLE 1. Chemical composition of the essential oil of *L. nobilis* leaves

No.	Component ^a	RT	RI ^b	Relative %	Mass fragments <i>m/z</i>		
					M ⁺ (<i>m/z</i>)	Base peak (<i>m/z</i>)	Other fragments
1	α -Thujene	7.16	909	0.04	136	93	121, 105, 77, 65, 43
2	α -Pinene	7.36	917	0.67	136	93	121, 105, 77, 67, 53, 41
3	Sabinene	8.59	961	1.80	136	93	121, 107, 77, 69, 53, 41
4	β -Pinene	8.66	964	0.38	136	41	121, 107, 93, 79, 69, 53
5	β -Myrcene	9.09	980	0.54	136	41	121, 107, 93, 79, 69, 53
6	α -Phellandrene	9.48	994	0.09	136	93	121, 105, 77, 65, 41
7	3-Carene	9.65	1000	0.38	136	93	121, 105, 77, 67, 41
8	α -Terpinene	9.87	1007	0.20	136	93	121, 105, 77, 65, 41
9	<i>P</i> -Cymene	10.13	1015	0.05	134	119	105, 91, 77, 65, 51, 36
10	1,8-Cineole	10.43	1025	27.41	154	43	140, 139, 125, 108, 84, 81, 69, 41
11	cis- β -Ocimene	10.58	1030	0.04	136	93	121, 105, 79, 67, 53, 41
12	trans- β -Ocimene	10.87	1039	0.27	136	93	121, 105, 79, 67, 53, 41
13	γ -Terpinene	11.19	1049	0.72	136	93	121, 105, 77, 65, 41
14	cis-Sabinene hydrate	11.44	1058	0.16	154	43	140, 136, 121, 111, 93, 71, 69, 41
15	Terpinolene	12.10	1079	0.34	136	93	121, 105, 79, 67, 41
16	Unknown	12.35	1087	0.02	-	43	142, 132, 117, 99, 85, 71, 58, 41
17	Linalool	12.59	1094	19.37	154	71	136, 121, 107, 93, 69, 43, 41
18	cis- <i>p</i> -Menth-2-en-1-ol	13.18	1113	0.08	154	43	139, 121, 111, 93, 79, 69, 41
19	trans- <i>p</i> -Menth-2-en-1-ol	13.74	1131	0.05	154	43	139, 121, 111, 93, 83, 69, 41
20	δ -Terpineol	14.57	1158	0.25	154	59	140, 136, 121, 107, 93, 81, 43, 41
21	Terpinen-4-ol	14.89	1169	2.09	154	71	140, 136, 121, 111, 93, 69, 43, 41
22	α -Terpineol	15.32	1182	2.84	154	59	140, 136, -121, 107, 93, 81, 43, 41
23	Linalool acetate	17.17	1245	0.25	196	93	182, 169, 150, 136, 121, 105, 80, 69, 43, 41
24	Unknown	17.29	1250	0.07	-	69	137, 123, 110, 82, 43, 41
25	Unknown	17.76	1266	0.39	-	92	194, 179, 165, 152, 134, 119, 105, 79, 65, 43, 41
26	Bornyl acetate	18.09	1277	0.18	196	95	136, 121, 108, 80, 67, 43, 41
27	Sabinyl acetate	18.27	1284	0.04	194	91	134, 119, 108, 77, 65, 43
28	(-)-trans-Pino-carvyl acetate	18.50	1292	0.04	194	43	119, 105, 91, 79, 65, 53, 41
29	δ -Terpinyl acetate	18.98	1309	0.79	196	43	136, 121, 101, 93, 80, 59, 41
30	δ -Elemene	19.53	1328	0.03	204	121	189, 175, 161, 147, 136, 107, 93, 79, 67, 41
31	Unknown	19.70	1334	0.23	-	43	195, 170, 152, 126, 108, 93, 69, 41
32	α -Terpinyl acetate	19.98	1344	14.65	196	121	136, 107, 93, 81, 59, 43, 41

TABLE 1. Cont.

No.	Component ^a	RT	RI ^b	Relative %	Mass fragments <i>m/z</i>		
					M ⁺ (<i>m/z</i>)	Base peak (<i>m/z</i>)	Other fragments
33	Eugenol	20.20	1351	1.56	164	164	149, 131, 121, 103, 91, 77, 65, 55
34	Neryl acetate	20.27	1354	0.79	196	69	136, 121, 107, 93, 80, 53, 43, 41
35	α -Copaene	20.65	1367	0.17	204	119	189, 161, 147, 133, 105, 91, 81, 65, 41
36	Geranyl acetate	20.81	1373	0.42	196	69	136, 121, 107, 93, 80, 41
37	β -Elemene	21.08	1382	0.98	204	93	189, 175, 161, 147, 133, 121, 107, 81, 67, 55, 41
38	Methyl eugenol	21.51	1397	7.73	178	178	163, 147, 135, 115, 107, 91, 77, 65, 51, 41
39	β -Caryophyllene	21.86	1410	0.16	204	41	189, 175, 161, 147, 133, 120, 105, 93, 79, 69, 55
40	α -Guaiene	22.33	1429	0.05	204	105	189, 175, 161, 147, 133, 121, 93, 79, 67, 55, 41
41	trans- Cinnamyl acetate	22.54	1437	0.55	176	43	147, 133, 115, 105, 92, 77, 63
42	α -Humulene	22.77	1446	0.18	204	93	161, 147, 136, 121, 107, 80, 67, 53, 41
43	Alloaromadendrene	22.97	1454	0.21	204	41	189, 175, 161, 147, 133, 119, 105, 91, 79, 67, 55
44	Unknown	23.14	1460	0.25	-	43	151, 136, 110, 95, 79, 69, 41
45	γ -Muurolene	23.34	1468	0.17	204	161	189, 175, 147, 133, 119, 105, 91, 79, 69, 55, 41
46	Germacrene D	23.49	1474	0.29	204	161	147, 133, 119, 105, 91, 81, 67, 55, 41
47	β - Selinene	23.63	1480	0.15	204	105	189, 175, 161, 147, 133, 121, 93, 79, 67, 55, 41
48	Unknown	23.74	1484	0.28	-	93	119, 107, 79, 69, 55, 41
49	Bicyclogermacrene	23.90	1490	0.94	204	121	189, 161, 147, 136, 107, 93, 79, 67, 55, 41
50	Unknown	24.04	1496	0.13	-	91	202, 187, 173, 159, 145, 131, 119, 105, 79, 69, 55
51	Germacrene A	24.13	1499	0.14	204	93	189, 178, 161, 147, 133, 119, 107, 79, 67, 55, 41
52	Cubebol	24.36	1508	0.22	222	161	207, 189, 179, 147, 133, 119, 105, 91, 81, 69, 43
53	Unknown	24.46	1512	0.14	-	122	189, 175, 161, 147, 133, 107, 93, 81, 67, 55, 41
54	δ - Cadinene	24.55	1515	0.58	204	161	189, 176, 145, 134, 119, 105, 91, 81, 69, 55, 41
55	Unknown	24.78	1525	0.06	-	119	189, 177, 161, 147, 133, 105, 91, 77, 69, 55, 41
56	α - Cadinene	24.92	1530	0.02	204	105	189, 175, 161, 149, 133, 119, 91, 81, 69, 55, 41
57	Elemol	25.21	1541	0.15	222	59	204, 189, 161, 147, 135, 121, 107, 93, 81, 43
58	Elemicin	25.38	1548	2.08	208	208	193, 177, 165, 150, 133, 118, 105, 91, 77, 65, 53
59	Unknown	25.72	1561	0.08	-	111	204, 189, 179, 161, 147, 135, 122, 93, 81, 67, 55
60	Spathulenol	25.97	1571	0.81	220	43	205, 187, 177, 159, 147, 131, 119, 105, 91, 79, 67, 41
61	Unknown	26.12	1577	0.36	-	43	204, 187, 177, 159, 147, 133, 121, 107, 91, 81, 69, 41

TABLE 1. Cont.

No.	Component ^a	RT	RI ^b	Relative %	Mass fragments <i>m/z</i>		
					M ⁺ (<i>m/z</i>)	Base peak (<i>m/z</i>)	Other fragments
62	Viridiflorol	26.33	1585	0.43	222	43	204, 189, 175, 161, 147, 133, 122, 109, 93, 81, 69, 41
63	Unknown	26.48	1591	0.04	-	120	202, 179, 159, 145, 138, 109, 93, 80, 69, 43
64	Unknown	26.61	1596	0.36	-	43	222, 204, 189, 179, 161, 147, 133, 122, 109, 93, 69, 43
65	Unknown	26.75	1602	0.07	-	43	205, 193, 177, 150, 138, 121, 109, 93, 79, 67, 41
66	1,10-di-epi-Cubenol	26.86	1606	0.07	222	43	204, 189, 179, 161, 147, 135, 119, 105, 95, 81, 67, 41
67	10-epi- γ - Eudesmol	27.01	1613	0.11	222	161	204, 189, 175, 149, 133, 119, 105, 91, 81, 59, 43, 41
68	1-epi- Cubenol	27.17	1620	0.26	222	119	204, 191, 179, 161, 149, 135, 105, 93, 81, 69, 41
69	τ -Muurolol	27.50	1634	0.63	222	95	204, 189, 179, 161, 149, 134, 121, 105, 81, 69, 43, 41
70	α -Muurolol	27.60	1639	0.17	222	161	204, 189, 177, 147, 133, 119, 105, 93, 81, 67, 43
71	Unknown	27.74	1645	0.53	222	-	208, 193, 164, 149, 133, 122, 108, 93, 79, 41
72	α -Cadinol	27.81	1648	1.42	222	95	204, 189, 161, 148, 137, 121, 109, 81, 69, 43
73	Unknown	28.18	1664	0.19	-	41	187, 177, 149, 137, 121, 107, 95, 81, 67, 55, 41
74	Unknown	28.27	1668	0.18	-	159	220, 202, 187, 174, 131, 119, 105, 81, 59, 41
75	Unknown	28.40	1673	0.07	-	189	220, 202, 177, 161, 147, 131, 119, 107, 95, 79, 67, 41
76	Eudesma-4(15),7-dien-1- β -ol	28.58	1681	0.15	220	109	202, 187, 177, 159, 149, 131, 117, 91, 79, 67, 41
77	Shyobunol	28.70	1687	0.99	222	84	204, 189, 161, 137, 121, 109, 81, 67, 55, 41
78	Unknown	29.09	1704	0.07	-	133	220, 202, 187, 177, 159, 145, 119, 105, 93, 79, 67, 41
79	Unknown	29.47	1720	0.09	-	41	220, 205, 187, 177, 159, 145, 131, 119, 105, 93, 79, 55
80	Unknown	29.64	1727	0.01	-	80	219, 203, 149, 137, 121, 109, 93, 79, 67, 41
81	Unknown	30.18	1751	0.08	-	43	202, 187, 173, 159, 145, 131, 119, 105, 91, 79, 67

^a Compounds are listed in order of their elution from a Rtx®-5MS column.

^b RI, linear retention indices on Rtx®-5MS column, experimentally determined using homologous series of n-alkanes (C8–C24). RT, retention time; *m/z*, mass to charge ratio.

Our results showed some variations with a previous study reported by El-Sawi et al. (2009), like decrease in percentage of major oil component 1,8-cineole, the variation in the percentage of other oil components including α -terpineol, neryl acetate, terpinen-4-ol and α -terpinyl acetate and the appearance of some oil constituents as linalool, α -cadinol, eugenol, methyl eugenol and elimicin. This large variation in the oil components and their percentage ensures the fact that collection time (season) affect metabolism of the plants (Hudaib et al., 2002; Luo et al., 2003; Kavoosi & Rowshan, 2013; Verma et al., 2013).

Moreover, the obtained data showed that the percentage of the studied leaf essential oil components differ from those previously reported in *L. nobilis* from other geographical regions. In fact, the concentration of 1,8- cineole in our study was lower than values recorded in *L. nobilis* from Cyprus (58.59%) (Yalçın et al., 2007), Turkey (41.1%) (Tomar et al., 2020), Bulgaria (41.02%) (Fidan et al., 2019) and Morocco (40.85%) (Nafis et al., 2020). However, the concentration of 1,8-cineole was higher compared to Tunisia (24.55%) (Mediouni Ben Jemâa et al., 2012) and Mauritius (4.15%) (Aumeeruddy-Elalfi et al., 2015) and was found to be similar to those in Russian oil (27.95%) (Riabov et al., 2020).

Besides geographical region, studies have shown differences in chemical profile and percentage of the main constituents between the oil obtained from young and old leaves (Kilic et al., 2004). 1,8- Cineole was the major component in both oils, but its concentration varied greatly between the young and old leaf (32.1% and 24.2%, respectively), that is in addition to the variation in the composition between the two oils' components. In general, we can say that, there are many factors that may affect the essential oil and may cause a great variation in its chemical composition, such as geographical area, climate, soil composition, stage of plant development, genotype, season of collection, drying and/or extraction method (Caredda et al., 2002; Flamini et al., 2007; Sellami et al., 2011; Morcia et al., 2012; Fadli et al., 2016; Hajdari et al., 2016; Taban et al., 2018; Elhidar et al., 2019; Nafis et al., 2019).

Cytotoxic activity of Laurus nobilis essential oil
L. nobilis leaves' essential oil exhibited a

potent inhibitory effect against *Hep-G2* cell line ($IC_{50}=1.83\pm 0.17\mu\text{g/mL}$) in comparison with standard vinblastine sulfate ($IC_{50}=2.93\mu\text{g/mL}$), and the cytotoxic effect increased in a dose dependent manner. Percentage of cell viability of *Hep-G2* cells treated with different concentrations of the essential oil is illustrated in Fig. 2.

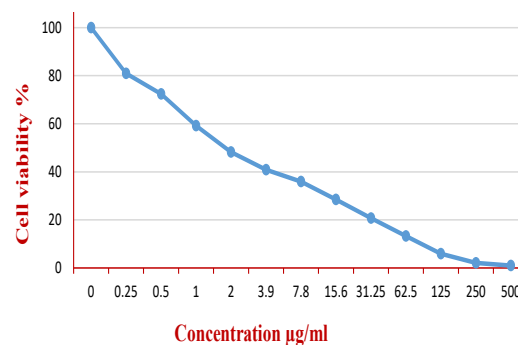


Fig. 2. Percentage of viable *Hep-G2* cells treated with different concentrations of essential oil from *L. nobilis* leaves

Molecular docking of Laurus nobilis essential oil components to Caspase3

Caspase3 is one of the caspase group of enzymes that initiate apoptosis in cancer cells including *Hep-G2* (Dong et al., 2018). In this molecular docking study, we aimed to figure out the essential oil components that can trigger stimulation of caspase3 and consequently initiate apoptosis of *Hep-G2*. The docking results showed that 32 of the identified oil components were able to form interactions with amino acids responsible for caspase3 activity (Table 2). The interactions include formation of hydrogen bonds, arene-arene hydrophobic and arene-cation interactions. In brief, some aromatics exhibited the best scores like elemicin that showed the minimum bonding energy (-14.307169) with Asn208, Trp214 and Phe250 and trans-cinnamyl acetate that formed four bonds with Arg64, Gln161, Trp206 and Arg207 at energy (-13.495376) (Fig. 3A). 1,8-Cineole (the major oil component) was able to dock with Asn208 with energy (-7.3826933) (Fig. 3A), which means that, it has a role in the cytotoxic activity but not the upper hand. Other components that exhibited interesting interactions are the oxygenated monoterpenes including linalool with Phe250 (E: -11.557581), cis-p-menth-2-en-1-ol with Arg64 and Arg207 (E: -10.418171), α -terpineol with Arg207 (E: -9.5154829), (-)-trans-pinocarvyl acetate with Arg207 (E: -13.335469) and linalool acetate with Ser209 (E: -10.784316) (Fig. 3B, Table 2) and the aromatics like eugenol with Asn208 (E:

-9.9296322) and methyl eugenol with His121 and Arg207 (E: -5.2686958) (Fig. 3C). Moreover, all of the oxygenated sesquiterpenes except 1,10-di-epi-cubenol were able to dock with one of the following amino acids; Arg207, Asn208, Glu246 and Phe250, 10-epi- γ - eudesmol exhibited the lowest binding energy from this group (-12.463281) (Fig. 3C).

From the docking results (Table 2), it can be postulated that the cytotoxic activity of essential oil of *L. nobilis* leaves is attributed to its high contents from oxygenated monoterpenes, aromatic compounds and oxygenated sesquiterpenes. This hypothesis is in agreement with data reported from literature. For example, 1,8-cineole suppressed the proliferation of human colorectal (*HCT116* and *RKO*) and ovarian (*A2780*) cancer cells by inducing apoptosis (Murata et al., 2013; Abdalla et al., 2020). Linalool has good inhibitory effects against breast, colorectal and liver cancer cells with IC_{50} values (224 μ M, 222 μ M, and 290 μ M, respectively) (Chang & Shen, 2014). Also, linalool exhibited strong cytotoxic activity against human skin cells *in vitro* (*HMEC-1*, *HNDf* and *153BR*) (Prashar et al., 2004). α - Terpineol showed significant cytotoxicity against *Hep-G2*, *HeLa*, *MOLT-4*, *K-562*, and *CTVR-1* human tumor cells (Hayes et al., 1997). Ho et al. reported that, eugenol demonstrated a cytotoxic effect to osteoblastic cell line *U2OS* in a dose-dependent manner with IC_{50} = 0.75 mmolL⁻¹ (Ho et al., 2006). Moreover, α -cadinol and τ -muurolol have been reported to have strong cytotoxic activity against *A-549* lung carcinoma, *MCF-7* breast adenocarcinoma and *HT-29* colon adenocarcinoma cell lines (Chang et al., 2000), while α - pinene presented some degree of cytotoxic activity against *A-549* and *HeLa* cell lines (CD_{50} values= 183.2 and 172.7 μ g/mL, respectively) (Silva et al., 2007). Sesquiterpenes have been found to be responsible for the cytotoxicity of *C. peregrine* essential oil against human lung carcinoma *A549* and colon adenocarcinoma *DLD-1* cell lines (Sylvestre et al., 2007). α - Humulene inhibited growth of tumor cells in *RAW264.7* and *HCT-116* cell lines (El Hadri et al., 2010).

Nonetheless, many studies have found that the oil is more potent than its single components against the tested cancer cell lines (Prashar et al., 2006; Silva et al., 2007; Dar et al., 2011; Döll-Boscardin et al., 2012). In addition to the complex composition of the essential oil, and the low concentration of its most components which make it difficult to attribute the high cytotoxic activity of

the oil to a single compound. For that we believe that, the most accepted hypothesis for explaining the high cytotoxicity of the oil is the synergism between the main components and the other cytotoxic active constituents.

Macromorphology of Laurus nobilis leaves and stem

The leaves (Fig. 4) are simple, shiny, glabrous, olive-green to dark green on the upper surface, dull olive on the lower surface, oblong or oblong-lanceolate in shape with acute to acuminate apices, entire margin, cuneate base, petiolate and the stipule is absent.

The midrib is elevated with reticulate venation. The leaves are alternate to opposite or apparently whorled.

The stem is formed of erect, cylindrical, woody trunk and numerous monopodial branches. The outer surface of the trunk and large branches is pale grey or greyish-brown in colour with fibrous fracture. The young stems and the terminal branches are thinner, angular with green glabrous outer surface.

Micromorphology of Laurus nobilis leaves, petioles and stems

Micromorphology and isolated elements of the leaf

The transverse section and isolated elements of the leaf are shown in Figs. 5, 6 and their measurements are summarized in Tables 3, 4. The section shows upper and lower epidermis free from covering trichomes. The lamina has dorsiventral structure with 2-3 rows of an upper palisade being discontinuous in the midrib region. The midrib is prominent on both sides but more prominent on the lower surface and shows a parenchymatous cortex with subepidermal collenchyma under both surfaces and is traversed by crescent shape collateral vascular bundle which is formed of xylem directed towards adaxial side and phloem directed towards the abaxial one. The pericycle is formed of patches of lignified fibers accompanied with sclereids.

The upper and lower epidermis of lamina (Fig. 5B, 6A, 6B) are formed of polygonal cells with sinuous and wavy moderately thick beaded anticlinal walls, covered with moderately thick smooth cuticle (Metcalf & Chalk, 1950).

TABLE 2. Molecular docking of *Laurus nobilis* essential oil components to Caspase3

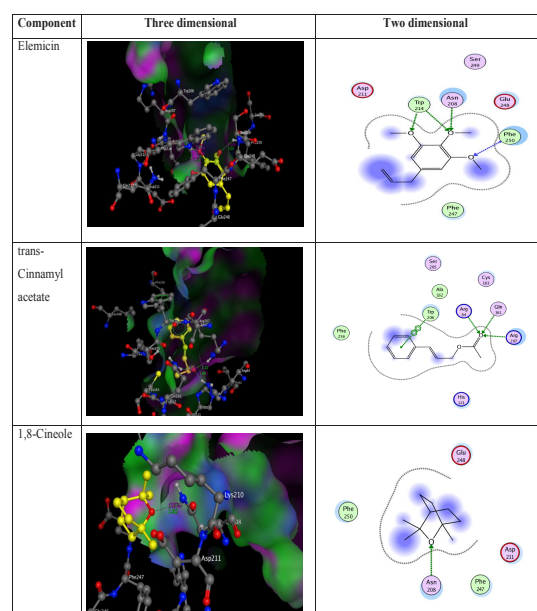
Compound	Score	Amino acid interactions
α -Thujene	-9.0934563	FD
α -Pinene	-9.8915119	FD
Sabinene	-10.606336	FD
β -Pinene	-9.3133602	FD
β -Myrcene	-11.5717	FD
α -Phellandrene	-10.964415	FD
3-Carene	-9.7488871	FD
α -Terpinene	-11.262818	FD
P-Cymene	-9.4803133	Arg207
1,8-Cineole	-7.3826933	Asn208
cis- β -Ocimene	-11.775062	FD
trans- β -Ocimene	-13.599358	FD
γ -Terpinene	-10.518329	FD
cis-Sabinene hydrate	-8.8080072	Arg207
Terpinolene	-10.672423	FD
Linalool	-11.557581	Phe250
cis-p-Menth-2-en-1-ol	-10.418171	Arg64, Arg207
trans-p-Menth-2-en-1-ol	-10.27935	Arg207
δ -Terpineol	-9.183959	Arg207
Terpinen-4-ol	-10.191397	Glu248
α -Terpineol	-9.5154829	Arg207
Linalool acetate	-10.784316	Ser209
Bornyl acetate	-10.727111	Arg207
Sabinyl acetate	-10.609087	Ser209
(-)-trans-Pinocarvyl acetate	-13.335469	Arg207
δ -Terpinyl acetate	-12.967546	Gln217
δ -Elemene	-10.91041	FD
α -Terpinyl acetate	-11.58408	Glu248
Eugenol	-9.9296322	Asn208
Neryl acetate	-10.401546	FD
α -Copaene	-12.61065	Arg64, Arg207
Geranyl acetate	-13.404128	Ser209
β - Elemene	-11.951816	FD
Methyl eugenol	-5.2686958	His121, Arg207
β -Caryophyllene	-12.48477	FD
α - Guaiene	-12.981331	FD
trans- Cinnamyl acetate	-13.495376	Arg64, Gln161, Trp206, Arg207
α -Humulene	-12.845993	FD
Alloaromadendrene	-10.839101	FD

TABLE 2. Cont.

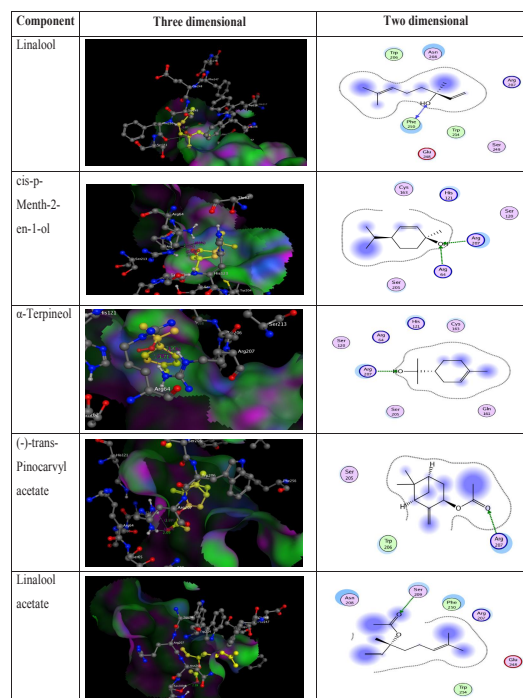
Compound	Score	Amino acid interactions
γ -Muurolene	-11.478368	FD
Germacrene D	-10.811728	FD
β - Selinene	-12.397589	FD
Bicyclogermacrene	-11.348759	FD
Germacrene A	-11.610316	FD
Cubebol	-9.186965	Ser209
δ - Cadinene	-12.624852	FD
α - Cadinene	-10.911288	FD
Elemol	-4.9086566	Asn208
Elemicin	-14.307169	Asn208, Trp214, Phe250
Spathulenol	-11.272525	Arg207
Viridiflorol	-6.4923453	Phe250
1,10-di-epi-Cubebol	2.0531795	Unfavorable binding
10-epi- γ - Eudesmol	-12.463281	Arg207
1-epi- Cubebol	-10.769084	Glu246
τ -Muurolol	-11.777497	Arg207
α -Muurolol	-8.5640545	Asn208
α -Cadinol	-11.662193	Arg207
Eudesma-4(15),7-dien-1- β -ol	-11.270865	Arg207
Shyobunol	-6.4838772	Asn208

FD fail to dock.

A) Compounds with lowest binding energy, highest number of bonds, major oil component.



B) Oxygenated monoterpenes representatives.



C) Aromatics and oxygenated sesquiterpene representatives

Component	Three dimensional	Two dimensional
Eugenol		
Methyl eugenol		
10-epi-γ-Eudesmol		

Key for two dimensional interactions generated by MOE;

- polar
- acidic
- basic
- greasy
- proximity
- contour
- sidechain acceptor
- sidechain donor
- backbone acceptor
- backbone donor
- ligand exposure
- solvent residue
- metal complex
- solvent contact
- metal contact
- receptor contact
- ⊗ arene-arene
- ⊕ arene-cation

Fig. 3. Representative examples for molecular docking of *Laurus nobilis* essential oil components to Caspase3.



Fig. 4. A photograph of *L. nobilis* leaves (x0.5)

The upper and lower neural epidermis (Fig. 5C, 6C, 6D) are polygonal, axially elongated with straight or beaded moderately thick anticlinal walls and covered with smooth moderately thick cuticle.

The stomata are limited only to the lower surface of the lamina. They are partially sunken below the plane of the epidermis (Metcalf & Chalk, 1950). The stomata (Fig. 6B) are oval to round in shape and of anomocytic type.

Trichomes are absent.

The mesophyll (Fig. 5B) is dorsiventral with an upper palisade layer being discontinuous in the midrib region and a moderately wide spongy tissue. The palisade layer (Fig. 5B) consists of 2-3 rows of cylindrical columnar cells with straight anticlinal walls.

The spongy tissue (Fig. 5B) formed of 5-7 rows of thin walled, more or less rounded parenchymatous cells with large intercellular spaces. Numerous rounded oil cells (Fig. 5B, 6E) are scattered in between the parenchyma cells of the sponge tissue. Oil cells are large, rounded, thin-walled and filled with yellowish essential oil.

The cortical tissue in the midrib region (Fig. 5C) is parenchymatous with subepidermal collenchyma under the upper and lower epidermis in 3-5 and 2-3 layers, respectively. The collenchymatous cells are more or less rounded with moderately thick cellulosic walls. They are followed by multilayered parenchymatous region of more or less rounded cells with thin cellulosic walls and narrow intercellular spaces. The endodermis is undistinguished.

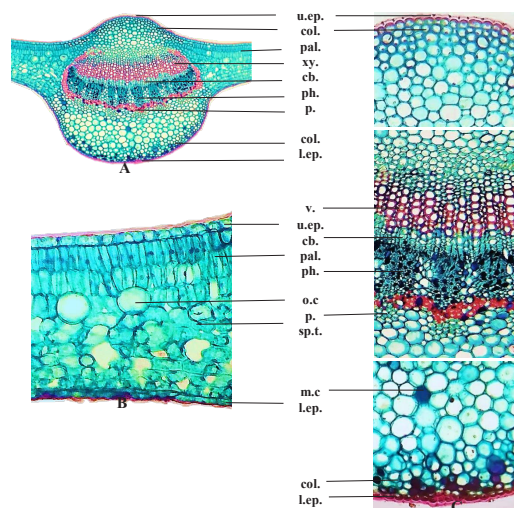


Fig. 5. Transverse section of the leaf: A- Photo of transverse section of the leaf (x32) (low power), B- Photo of detailed transverse section of the lamina (x112) (high power), C- Photo of detailed transverse section of the midrib (x136) (high power) [cb., cambium; col., collenchyma; Lep., lower epidermis; m.c., mucilage cell; o.c., oil cell; pal., palisade; p., pericycle; ph., phloem; sp.t., spongy tissue; u.ep., upper epidermis; v., vessel; xy., xylem]

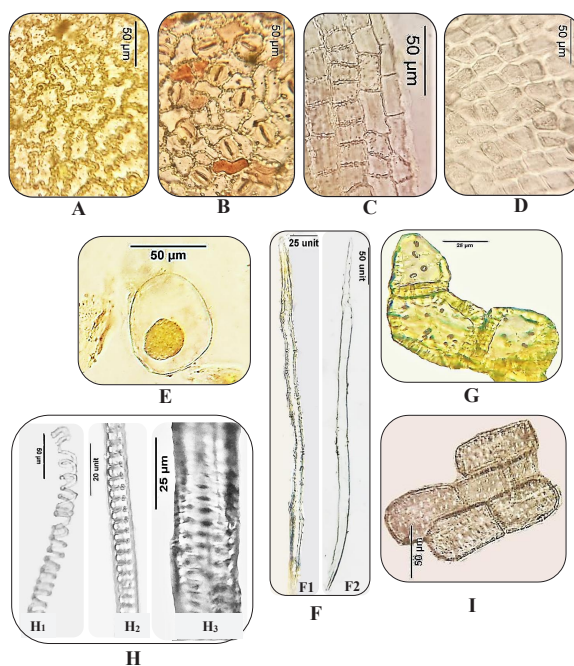


Fig. 6. Isolated elements of the leaf; A; upper epidermis of lamina (x220), B; lower epidermis of lamina (x230), C; upper neural epidermic (x350), D; lower neural epidermis (x230), E; oil cell (x410), F; fibers (x320 F1, x180 F2), G; sclereids (x520), H; vessels (x220 H1, x650 H2, x680 H3), I; pitted parenchyma (x260)

TABLE 3. The microscopical numerical values of the leaves of *L. nobilis*

Feature examined	Min-Max	mean±SD
Stomatal Index of the lower epidermis	15-19	2
Vein-Islet Number	5-6	0.5
Veinlet-Termination Number	1-2	0.5
Palisade Ratio	1.5-2.25	0.38

The pericycle (Fig. 5C) is formed of patches from lignified fibers accompanied with lignified sclereids. Fibers (Fig. 6F) are spindle-shape, with acute apices and moderately thick lignified walls showing few projections (dentate-like). The sclereids (Fig. 6G) are rectangular with U-shape thickened lignified walls (Metcalfe & Chalk, 1950).

The vascular tissue is recognized as crescent shape open collateral vascular bundles which is composed of an inner phloem, outer xylum and cambium in-between. The phloem (Fig. 5C) is focused to the downward side and is composed of polygonal thin-walled cellulosic parenchyma, sieve tubes and companion cells. The cambium (Fig. 5C) between xylum and phloem is formed from 5-7 layers. The xylem (Fig. 5C) is formed of radially elongated, moderately thick-walled lignified spiral, annular and pitted vessels (Fig. 6H) focused to the upward side, separated by thin wall cellulosic wood parenchyma.

Numerous mucilage cells (Fig. 5C) are observed in the cortex, pericycle and phloem. These cells gave dark blue colour after staining with methylene blue. The microscopical numerical values of the leaf are summarized in Table 3.

Micromorphology and isolated elements of the petiole

The transverse section and isolated elements of the petiole are illustrated in (Figs. 7, 8 and their measurements are mentioned in Table 4. The section is almost rounded in shape. It shows an outer epidermis surrounding a cortex formed of an outer collenchyma and inner parenchyma with numerous scattered oil and mucilage cells. The endodermis is distinguishable. The vascular tissue is formed of collateral crescent shape vascular bundle of phloem, cambium, xylem and surrounded by patches of thin-walled non-lignified pericyclic fibers.

TABLE 4. Microscopical measurements (in microns) of the leaf, petiole, young and old stem of *L. nobilis*

Element	Length	Width	Height	Diameter
Leaf				
Upper epidermis of lamina	25-54	14-22	9-13	--
Lower epidermis of lamina	16-47	11-27	6-11	--
Upper neural epidermis	16-32	10-18	9-14	--
Lower neural epidermis	21-36	12-21	7-11	--
Stomata	19-30	15-22	--	--
Palisade cells	24-33	6-12	--	--
Spongy parenchyma	--	--	--	13-32
Oil cells	--	--	--	26-48
Sub-epidermal collenchyma	--	--	--	5-16
Cortical parenchyma	--	--	--	11-50
Pericyclic fibers	370-982	13-22	--	--
Pericyclic sclereids	28-76	21-40	--	--
Xylem vessels	--	--	--	9-21
Mucilage cells	--	--	--	4-32
Petiole				
Epidermis	20-35	13-23	1-17	--
Hypodermal collenchyma	--	--	--	11-21
Cortical parenchyma	--	--	--	8-45
Oil cells	--	--	--	18-30
Pericyclic fibers	289-861	10-19	--	--
Xylem vessels	--	--	--	6-25
Mucilage cells	--	--	--	6-36
Young stem				
Epidermis	21-39	9-13	13-17	--
Stomata	23-37	17-24	--	--
Glandular hair	17-33	5-9	--	--
Non-glandular hair	27-103	4-11	--	--
Collenchyma cells	--	--	--	13-30
Cortical parenchyma cells	--	--	--	12-47
Oil cells	--	--	--	8-29
Pericyclic fibers	140-290	3-12	--	--
Xylem vessels	--	--	--	7-14
Wood parenchyma	35-79	24-60	--	--
Pith	--	--	--	18-64
Old stem				
Cork cells	21-57	17-30	5-11	--
Phellogen	15-24	5-10	--	--
Phelloderm	18-35	8-19	--	--
Oil cells	--	--	--	30-67
Pericyclic fibers	533-1163	12-47	--	--
Pericyclic sclereids	9-72	6-37	--	--
Xylem vessels	--	--	--	16-65
Wood parenchyma	31-90	24-60	--	--
Wood fibers	141-974	5-22	--	--
Tracheids	75-152	13-24	--	--
Pith	--	--	--	36-104

The epidermis of the petiole (Figs. 7B, 8A) are polygonal, with almost straight anticlinal walls and covered with thick smooth cuticle

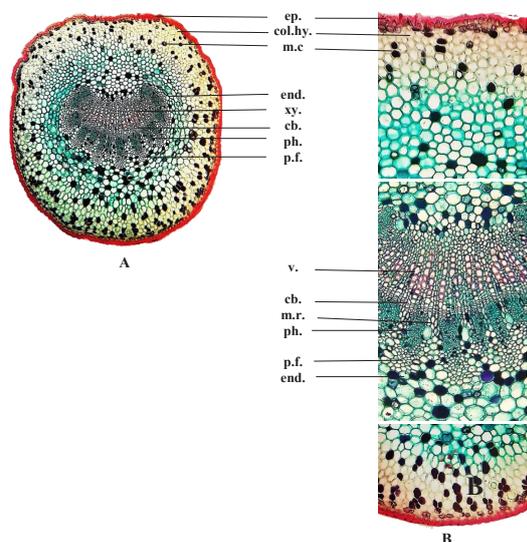


Fig. 7. A; Photo of transverse section of the petiole (x34) (low power), B; photo of detailed transverse section of the petiole (x74) (high power) [cb., cambium; col.hy., collenchymal hypodermis; c.par., cortical parenchyma; end., endodermis; ep., epidermis; m.c., mucilage cell; m.r.; medullary ray, p.f., pericyclic fiber; ph., phloem; v., vessel; xy., xylem]

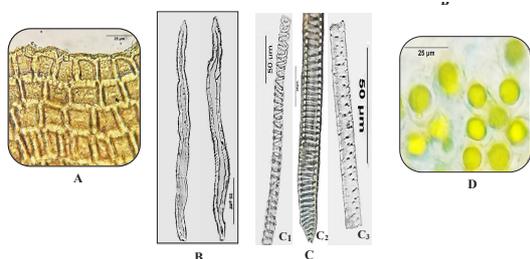


Fig. 8. Isolated elements of the petiole; A; epidermis (x320), B; fibers (x500), C; vessels (x250 C1, x460 C2, x570 C3), D; oil cells (x520)

Cortical tissue of the petiole (Fig. 7B) is parenchymatous with a continuous layer of 1-5 rows of collenchyma below the epidermis. The collenchymatous cells are angular with moderately thick cellulosic walls. The rest of the cortex is parenchymatous consisting of 7-13 rows of more or less rounded cells with narrow intercellular spaces. The endodermis is formed of axially elongated cells free from contents.

The pericycle (Fig. 7B) is formed of patches of fibers. Fibers (Fig. 8B) are spindle-shaped, with acute apices and moderately thick non-lignified walls.

The vascular tissue is formed of continuous, collateral, crescent shape vascular bundle, which consists of phloem to the downward, xylem to the upward and cambium in between.

The phloem (Fig. 7B) is composed of polygonal thin walled cellulosic parenchyma, sieve tubes and companion cells.

The cambium (Fig. 7B) consists of 4-7 rows of thin-walled tangentially elongated cellulosic meristematic cells.

The xylem (Fig. 7B) is formed of radially elongated moderately thick wall lignified vessels of spiral, annular and pitted type (Fig. 8C) and cellulosic wood parenchyma.

The medullary rays (Fig. 7B) are uni- to tetraseriate; the cells are more or less rounded in the phloem region and rectangular, radially elongated in the xylem region; they have moderately thin cellulosic walls.

Numerous oil (Figs. 7B, 8D) and mucilage cells (Fig. 7B) are scattered in the cortex, phloem parenchyma and medullary ray, similar to that in the leaf.

Micromorphology and isolated elements of the Stem

The transverse sections in the young and old stems and their measurements are shown in Figs. 9, 10, 11, 12 and Table 4. As to the young stem, it is almost triangular to heart-shape in outline. It shows an outer epidermis followed by collenchymatous hypodermis and wide parenchymatous cortex. The endodermis is distinguished as a single row of tangentially elongated cells surrounding each vascular bundle. The vascular tissue is formed of separated vascular bundles surrounding a wide parenchymatous pith, and the vascular bundle consists of phloem and xylem underneath. A band of non-lignified pericyclic fibers is abutting over the vascular bundles.

A transverse section of the old stem (Fig. 10) is circular in outline. It shows an outer layer of

cork followed by phellogen and phelloderm. The pericycle is formed of patches of lignified fibers interrupted with groups of lignified sclereids to form a continuous ring. The vascular tissue is formed of a continuous ring of an outer

phloem, inner xylem and cambium in between. The vascular tissue is transversed by numerous medullary rays and surrounding narrow parenchymatous pith.

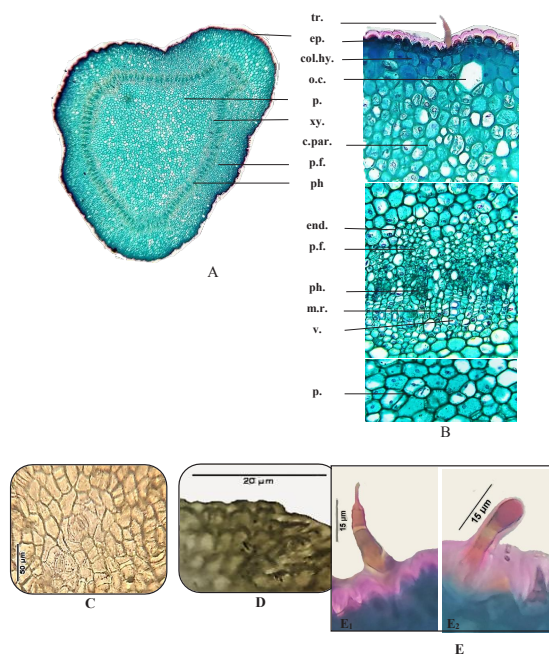


Fig. 9. A; photo of transverse section of the young stem (x74), B; photo of detailed transverse section of the young stem (x714), C; epidermis (x200), D; papillose epidermis (x1750), E; trichomes (x700 E1, x967 E2) [col.hy., collenchymatous hypodermis; c.par., cortical parenchyma; end., endoderms; e.p., epidermis; m.r., medullary rays; o.c., oil cell; p., pith; p.f., pericyclic fiber; ph., phloem; tr.; trichome, v., vessel; xy., xylem]

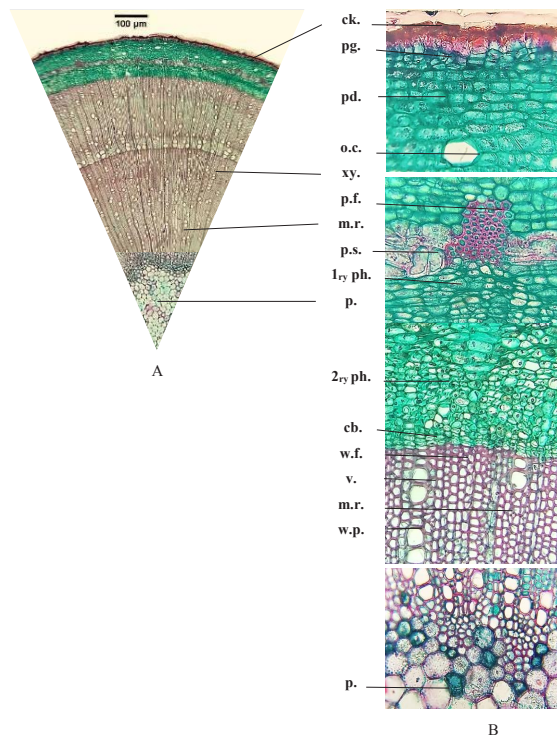


Fig. 10. A; photo of transverse section of the old stem (x90), B; photo of detailed transverse section of the old stem (x1022) [cb., cambium; ck., cork; m.r., medullary rays; o.c., oil cell; p., pith; pd., phelloderm; p.f., pericyclic fiber; pg., phellogen; 1ry ph., primary phloem; 2ry ph., secondary phloem; p.s., pericyclic scleried; v., vessel; w.f., wood fiber; w.p., wood parenchyma; xy., xylem]

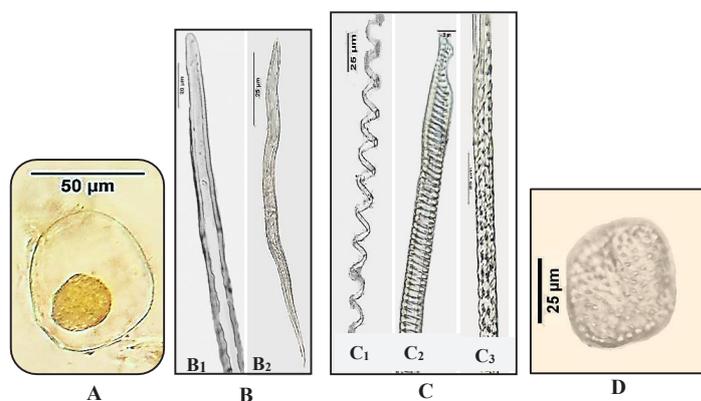


Fig. 11. Isolated elements of the young stem; A; oil cell (x380), B; fibers (x400 B1, x460 B2), C; vessels (x200 C1, x220 C2, x450 C3), D; pitted parenchyma (x400)

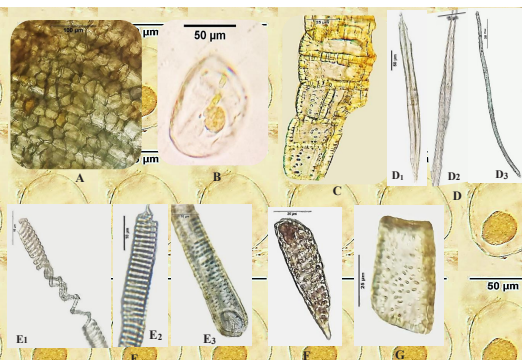


Fig. 12. Isolated elements of the old stem; **A**; cork cells (x130), **B**; oil cells (x290), **C**; sclereids (x360), **D**; fibers (x120 **D1**, x533 **D2**, x320 **D3**), **E**; vessels (x900 **E1**, x800 **E2**, x800 **E3**), **F**; tracheid (x440), **G**; pitted wood parenchyma (x520)

The epidermal cells of the young stem (Figs. 9B, 9C) are polygonal, papillosed (Fig. 9D), axially elongated and covered with thick smooth cuticle. Stomata (Fig. 9C) are present on the epidermis of the young stem. They are similar to that of the leaf.

Trichomes (Figs. 9B, 9E) are few, they are of both glandular and non-glandular types. The non-glandular trichomes are unicellular and multicellular uniseriate 3 cells with acute apex. The glandular trichomes are with unicellular head and unicellular stalk.

The cortex in the young stem (Fig. 9B) is formed of 1-2 rows of more or less rounded collenchymatous hypodermal cells with moderately thick cellulose walls, followed by 11-15 rows of more or less rounded parenchymatous cells with small intercellular spaces.

The cork of the old stem (Figs. 10B, 12A) is formed of 1-2 rows of polygonal cells with thick suberized walls and have brownish contents.

The phellogen (Fig. 10B) is formed of 2-3 rows of elongated rectangular parenchyma cells.

The phelloderm in the old stem (Fig. 10B) is formed of 7-13 rows of rectangular parenchymatous cells with narrow intercellular spaces. The cortex in the young stem and the phelloderm in the old stem are limited in the inner side by axially elongated endodermal cells free of any contents.

The pericycle in the young stem (Fig. 9B) is parenchymatous with patches of non-lignified fibers abutting the vascular bundles. The pericyclic fibers (Fig. 11B) are spindle-shaped, with tapering ends and thin non-lignified walls. In the old stem, the pericycle (Fig. 10B) is formed of patches of lignified fibers interrupted with lignified groups of moderately-thick sclereids to form continuous ring. The pericyclic fibers (Fig. 12D) are spindle-shaped, with tapering ends, wide lumen and thin lignified walls. The sclereids (Fig. 12C) have U-shape thickening with thin outer tangential wall and thick sclerosed inner tangential and radial walls (Metcalf & Chalk, 1950).

The vascular tissue in the young stem (Fig. 9A) is formed of separated vascular bundles surrounding central pith and separated by medullary rays. Each vascular bundle consists of an outer phloem and inner xylem. In the old stem, the vascular tissue (Fig. 10A) is formed of a continuous ring of an outer phloem and an inner xylem showing cambium in-between and transversed by medullary rays.

The phloem in the young stem (Fig. 9B) is formed of thin walled cellulose parenchymatous cells, sieve tubes and companion cells. In the old stem, (Fig. 10B), the primary phloem consists of thin walled parenchyma and ceratenchyma, while the secondary phloem consists of polygonal thin-walled cellulose parenchyma, sieve tubes and companion cells.

The cambium in the young stem is not well differentiated. In the old stem (Fig. 10B), it consists of 3-5 rows of tangentially elongated thin-walled cellulose meristematic cells.

The xylum (Figs. 9B, 10B) consists of alternative bands of lignified wood parenchyma, wood fibers and xylem vessels in which they are present isolated or in groups of 2-5. The vessels (Figs. 11C, 12E) are lignified, with spiral, pitted and annular thickening.

The wood fibers (Fig. 12D) are in groups of radial rows, spindle-shape with moderately thick lignified walls, relatively narrow lumens and rounded apices.

The tracheids (Fig. 12F) are elongated with blunt apices and lignified pitted walls.

The wood parenchyma (Fig. 12G) are para-tracheal and consists of polygonal to rectangular pitted cells with thin, slightly lignified walls.

The medullary rays (Figs. 9B, 10B) are mostly uni- to bi-seriate and formed of cellulose, rectangular, radially elongated cells.

The pith (Figs. 9B, 10B) is wide in the young stem and it is relatively narrow in the old stem. It is formed of large more or less rounded, thin-walled cellulose parenchyma cells with small intercellular spaces.

Numerous rounded to oval large, thin wall oil cells (Figs. 9B, 10B, 11A, 12B) filled with yellow essential oil are scattered in the parenchymatous cells of the cortex, medullary rays and pith. (Metcalf & Chalk, 1950).

Conclusion

GC/MS analysis of *Laurus nobilis* essential oil showed the presence of 81 compound from which 59 were identified based on comparison of their retention index with that reported in the literature with 1,8-cineole (27.41%) as major component. Besides that, comparing the essential oil contents with previous studies confirmed the effect of collection season and geographical source on the oil composition. Moreover, the current study revealed the potent inhibitory effect of the essential oil of *Laurus nobilis* on *Hep-G₂* cell line (IC₅₀=1.83 µg/ml) in comparison with standard vinblastine sulfate (IC₅₀ = 2.93 µg/ml). Molecular docking of the essential oil components to caspase3 highlighted the main oil subclasses that are responsible for activity including oxygenated monoterpenes, aromatics and oxygenated sesquiterpenes. A detailed microscopical examination of different organs of the plant is described to help in its identification in the powdered form.

Conflict of interest: The authors declare that, there is no conflict of interest.

Author contribution: N.N., Carried out all the practical part, analyzed the data and drafted the manuscript; I.M., Performed molecular docking, participated in data analysis and manuscript revision and provided supervision; G.D., Provided revision and supervision; Z. E-S., Participated in

data analysis and manuscript revision and provided supervision; A-M. A., Provided the research idea and supervision.

Ethical approval: Not applicable.

References

- Abdalla, A.N., Shaheen, U., Abdallah, Q., Flamini, G., Bkhaitan, M.M., et al. (2020) Proapoptotic activity of *Achillea membranacea* essential oil and its major constituent 1, 8-cineole against A2780 ovarian cancer cells. *Molecules*, **25**(7), 1582.
- Abu-Dahab, R., Kasabri, V., Afifi, F.U. (2014) Evaluation of the volatile oil composition and antiproliferative activity of *Laurus nobilis* L. (Lauraceae) on breast cancer cell line models. *Records of Natural Products*, **8**(2), 136-147.
- Adams, R.P. (1995) "*Identification of Essential Oil Components by Gas Chromatography/Mass Spectroscopy*". Allured Publishing Corporation, Carol Stream, Illinois, U.S.A.
- Aumeeruddy-Elalfi, Z., Gurib-Fakim, A., Mahomoodally, F. (2015) Antimicrobial, antibiotic potentiating activity and phytochemical profile of essential oils from exotic and endemic medicinal plants of Mauritius. *Industrial Crops and Products*, **71**, 197-204.
- Caredda, A., Marongiu, B., Porcedda, S., Soro, C. (2002) Supercritical carbon dioxide extraction and characterization of *Laurus nobilis* essential oil. *Journal of Agricultural and Food Chemistry*, **50**(6), 1492-1496.
- Chang, M.-Y., Shen, Y.-L. (2014) Linalool exhibits cytotoxic effects by activating antitumor immunity. *Molecules*, **19**(5), 6694-6706.
- Chang, S.-T., Wang, D. S.-Y., Wu, C.-L., Shiah, S.-G., Kuo, Y.-H., et al. (2000) Cytotoxicity of extractives from *Taiwania cryptomerioides* heartwood. *Phytochemistry*, **55**(3), 227-232.
- Charles, D.J. (2013) "*In Antioxidant Properties of Spices, Herbs and Other Sources*", pp. 181-187. New York Springer Science + Buiseness Media.
- Dar, M.Y., Shah, W.A., Rather, M.A., Qurishi, Y., Hamid, A., et al. (2011) Chemical composition, *in vitro* cytotoxic and antioxidant activities of the

- essential oil and major constituents of *Cymbopogon jawarancusa* (Kashmir). *Food Chemistry*, **129**(4), 1606-1611.
- Döll-Boscardin, P.M., Sartoratto, A., Sales Maia, B.H.N., Padilha de Paula, J., Nakashima, T., et al. (2012) *In vitro* cytotoxic potential of essential oils of *Eucalyptus benthamii* and its related terpenes on tumor cell lines. *Evidence-Based Complementary and Alternative Medicine*, **2012**(4), 342652.
- Dong, N., Liu, X., Zhao, T., Wang, L., Li, H., et al. (2018) Apoptosis-inducing effects and growth inhibitory of a novel chalcone, in human hepatic cancer cells and lung cancer cells. *Biomedicine and Pharmacotherapy*, **105**, 195-203.
- El-Sawi, S.A., Ibrahim, M.E., Ali, A.M. (2009) *In vitro* cytotoxic, antioxidant and antimicrobial activities of essential oil of leaves of *Laurus nobilis* L. grown in Egypt and its chemical composition. *Medicinal and Aromatic Plant Science and Biotechnology*, **3**(1), 16-23.
- El Hadri, A., del Rio, M.G., Sanz, J., Coloma, A.G., Idaomar, M., et al. (2010) Cytotoxic activity of α -humulene and transcaryophyllene from *Salvia officinalis* in animal and human tumor cells. *Anales de la Real Academia Nacional de Farmacia*, **76**(3), 343-356.
- Elhidar, N., Nafis, A., Kasrati, A., Goehler, A., Bohnert, J.A., et al. (2019) Chemical composition, antimicrobial activities and synergistic effects of essential oil from *Senecio anteuphorbium*, a Moroccan endemic plant. *Industrial Crops and Products*, **130**, 310-315.
- Fadli, M., Pagès, J.-M., Mezrioui, N.-E., Abbad, A., Hassani, L. (2016) *Artemisia herba-alba* Asso and *Cymbopogon citratus* (DC.) Stapf essential oils and their capability to restore antibiotics efficacy. *Industrial Crops and Products*, **89**, 399-404.
- Fidan, H., Stefanova, G., Kostova, I., Stankov, S., Damyanova, S., et al. (2019) Chemical composition and antimicrobial activity of *Laurus nobilis* L. essential oils from Bulgaria. *Molecules*, **24**(4), 804.
- Flamini, G., Tebano, M., Cioni, P.L., Ceccarini, L., Ricci, A.S., et al. (2007) Comparison between the conventional method of extraction of essential oil of *Laurus nobilis* L. and a novel method which uses microwaves applied *in situ*, without resorting to an oven. *Journal of Chromatography A*, **1143**(1), 36-40.
- Gomha, S.M., Riyadh, S.M., Mahmmoud, E.A., Elaasser, M.M. (2015) Synthesis and anticancer activities of thiazoles, 1,3-thiazines, and thiazolidine using chitosan-grafted-poly (vinylpyridine) as basic catalyst. *Heterocycles*, **91**(6), 1227-1243.
- Hajdari, A., Mustafa, B., Nebija, D., Selimi, H., Veselaj, Z., et al. (2016) Essential oil composition of *Pinus peuce* Griseb. needles and twigs from two national parks of Kosovo. *The Scientific World Journal*, **2016**, 5393079.
- Hayes, A.J., Leach, D.N., Markham, J.L., Markovic, B. (1997) *In vitro* cytotoxicity of Australian Tea Tree Oil using human cell lines. *Journal of Essential Oil Research*, **9**(5), 575-582.
- Ho, Y.-C., Huang, F.-M., Chang, Y.-C. (2006) Mechanisms of cytotoxicity of eugenol in human osteoblastic cells in vitro. *International Endodontic Journal*, **39**(5), 389-393.
- Hudaib, M., Speroni, E., Di Pietra, A.M., Cavrini, V. (2002) GC/MS evaluation of thyme (*Thymus vulgaris* L.) oil composition and variations during the vegetative cycle. *Journal of Pharmaceutical and Biomedical Analysis*, **29**(4), 691-700.
- Kavoosi, G., Rowshan, V. (2013) Chemical composition, antioxidant and antimicrobial activities of essential oil obtained from *Ferula assa-foetida* oleo-gum-resin: Effect of collection time. *Food Chemistry*, **138**(4), 2180-2187.
- Kilic, A., Hafizoglu, H., Kollmannsberger, H., Nitz, S. (2004) Volatile constituents and key odorants in leaves, buds, flowers, and fruits of *Laurus nobilis* L. *Journal of Agricultural and Food Chemistry*, **52**(6), 1601-1606.
- Lee, E.H., Shin, J.H., Kim, S.S., Lee, H., Yang, S.R., et al. (2019) *Laurus nobilis* leaf extract controls inflammation by suppressing NLRP3 inflammasome activation. *Journal of Cellular Physiology*, **234**(5), 6854-6864.
- Luo, J., Liu, Y., Feng, Y., Guo, X., Cao, H. (2003) Two chemotypes of *Pogostemon cablin* and influence of region of cultivation and harvesting time on volatile oil composition. *Acta pharmaceutica Sinica*, **38**(4), 307.

- Mediouni Ben Jemâa, J., Tersim, N., Toudert, K.T., Khouja, M.L. (2012) Insecticidal activities of essential oils from leaves of *Laurus nobilis* L. from Tunisia, Algeria and Morocco, and comparative chemical composition. *Journal of Stored Products Research*, **48**, 97-104.
- Metcalf, C.R., Chalk, L. (1950) "Anatomy of Dicotyledons", Vol. II. Clarendon press, Oxford.
- Morcia, C., Malnati, M., Terzi, V. (2012) *In vitro* antifungal activity of terpinen-4-ol, eugenol, carvone, 1,8-cineole (eucalyptol) and thymol against mycotoxigenic plant pathogens. *Food Additives & Contaminants: Part A*, **29**(3), 415-422.
- Mosmann, T. (1983) Rapid colorimetric assay for cellular growth and survival: application to proliferation and cytotoxicity assays. *Journal of Immunological Methods*, **65**(1-2), 55-63.
- Moteki, H., Hibasami, H., Yamada, Y., Katsuzaki, H., Imai, K., et al. (2002) Specific induction of apoptosis by 1,8-cineole in two human leukemia cell lines, but not a in human stomach cancer cell line. *Oncology Reports*, **9**(4), 757-760.
- Murata, S., Shiragami, R., Kosugi, C., Tezuka, T., Yamazaki, M., et al. (2013) Antitumor effect of 1, 8-cineole against colon cancer. *Oncology Reports*, **30**(6), 2647-2652.
- Nafis, A., Kasrati, A., Jamali, C.A., Custódio, L., Vitalini, S., et al. (2020) A Comparative study of the *in vitro* antimicrobial and synergistic effect of essential oils from *Laurus nobilis* L. and *Prunus armeniaca* L. from Morocco with antimicrobial drugs: New approach for health promoting products. *Antibiotics*, **9**(4), 140.
- Nafis, A., Kasrati, A., Jamali, C.A., Mezrioui, N., Setzer, W., et al. (2019) Antioxidant activity and evidence for synergism of *Cannabis sativa* (L.) essential oil with antimicrobial standards. *Industrial Crops and Products*, **137**, 396-400.
- Nagah, N., Mostafa, I., Osman, A., Dora, G., El-Sayed, Z., et al. (2021) Bioguided isolation and in-silico analysis of Hep-G2 cytotoxic constituents from *Laurus nobilis* Linn. cultivated in Egypt. *Egyptian Journal of Chemistry*, **64**(5), 2731-2745.
- Ozcan, B., Esen, M., Sangun, M.K., Coleri, A., Caliskan, M. (2010) Effective antibacterial and antioxidant properties of methanolic extract of *Laurus nobilis* seed oil. *Journal of Environmental Biology*, **31**(5), 637-641.
- Patrakar, R., Mansuriya, M., Patil, P. (2012) Phytochemical and pharmacological review on *Laurus nobilis*. *International Journal of Pharmaceutical and Chemical Sciences*, **1**(2), 595-602.
- Prashar, A., Locke, I.C., Evans, C.S. (2004) Cytotoxicity of lavender oil and its major components to human skin cells. *Cell Proliferation*, **37**(3), 221-229.
- Prashar, A., Locke, I.C., Evans, C.S. (2006) Cytotoxicity of clove (*Syzygium aromaticum*) oil and its major components to human skin cells. *Cell Proliferation*, **39**(4), 241-248.
- Riabov, P.A., Micić, D., Božović, R.B., Jovanović, D. V., Tomić, A., et al. (2020) The chemical, biological and thermal characteristics and gastronomical perspectives of *Laurus nobilis* essential oil from different geographical origin. *Industrial Crops and Products*, **151**, 112498.
- Saab, A.M., Guerrini, A., Zeino, M., Wiench, B., Rossi, D., et al. (2015) *Laurus nobilis* L. seed extract reveals collateral sensitivity in multidrug-resistant p-glycoprotein-expressing tumor cells. *Nutrition and Cancer*, **67**(4), 664-675.
- Saeed, M.E.M., Meyer, M., Hussein, A., Efferth, T. (2016) Cytotoxicity of South-African medicinal plants towards sensitive and multidrug-resistant cancer cells. *Journal of Ethnopharmacology*, **186**, 209-223.
- Saleh, E.A., Al-Hawary, I.I., Elnajar, M.M. (2019) Antibacterial and anti-oxidant activities of laurel oil against *Staphylococcus aureus* and *Pseudomonas fluorescens* in *Oreochromis niloticus* filets. *Slovenian Veterinary Research*, **56**, 313-319.
- Sellami, I.H., Wannes, W.A., Bettaieb, I., Berrima, S., Chahed, T., et al. (2011) Qualitative and quantitative changes in the essential oil of *Laurus nobilis* L. leaves as affected by different drying methods. *Food Chemistry*, **126**(2), 691-697.
- Serebrynyaya, F.K., Nasuhova, N.M., Kononov, D.A. (2017) Morphological and anatomical study of the leaves of *Laurus nobilis* L. (Lauraceae), growing in the introduction of the northern Caucasus Region

- (Russia). *Pharmacognosy Journal*, **9**(4), 519-522.
- Silva, S.L., Figueiredo, P.M., Yano, T. (2007) Cytotoxic evaluation of essential oil from *Zanthoxylum rhoifolium* Lam. leaves. *Acta Amazonica*, **37**, 281-286.
- Sylvestre, M., Pichette, A., Lavoie, S., Longtin, A., Legault, J. (2007) Composition and cytotoxic activity of the leaf essential oil of *Comptonia peregrina* (L.) Coulter. *Phytotherapy Research*, **21**(6), 536-540.
- Taban, A., Saharkhiz, M.J., Niakousari, M. (2018) Sweet bay (*Laurus nobilis* L.) essential oil and its chemical composition, antioxidant activity and leaf micromorphology under different extraction methods. *Sustainable Chemistry and Pharmacy*, **9**, 12-18.
- Taoudiat, A., Djenane, D., Ferhat, Z., Spigno, G. (2018) The effect of *Laurus nobilis* L. essential oil and different packaging systems on the photo-oxidative stability of Chemlal extra-virgin olive oil. *Journal of Food Science and Technology*, **55**(10), 4212-4222.
- Tomar, O., Akarca, G., Gök, V., Ramadan, M.F. (2020) Composition and antibacterial effects of Laurel (*Laurus nobilis* L.) leaves essential oil. *Journal of Essential Oil Bearing Plants*, **23**(2), 414-421.
- Verma, R.S., Padalia, R.C., Chauhan, A. (2013) Volatile oil composition of Indian Perilla [*Perilla frutescens* (L.) Britton] collected at different phenophases. *Journal of Essential Oil Research*, **25**(2), 92-96.
- Yalçın, H., Anık, M., Şanda, M.A., Çakır, A. (2007) Gas chromatography/mass spectrometry analysis of *Laurus nobilis* essential oil composition of northern Cyprus. *Journal of Medicinal Food*, **10**(4), 715-719.

مكونات الزيت الطيار و التأثير المضاد للخلايا السرطانية للكبد و البصمة الظاهرية و المجهرية لنبات اللورا المنزرع في مصر

نسمة نجاج، إسلام مصطفى، جمال درة، زينب السيد، عبدالمنعم عطية
قسم العقاقير - كلية الصيدلة - جامعة الزقازيق - الزقازيق - 44519 - مصر.

أظهر تحليل كروماتوجرافيا الغاز المتصل بمطياف الكتلة للزيت الطيار المقطر مع الماء من الاوراق الطازجة لنبات اللورا المنزرع في مصر وجود 81 مكون تم التعرف على 59 منهم، وتمثل نسبة المواد التي تم التعرف عليها 96.3% من إجمالي نسبة المواد في الزيت الطيار. هذا وقد كانت المواد ذات النسبة الأكبر في تكوين الزيت الطيار هي 1-8 سنيول (22.47%)، لينالول (19.37%)، الفا-ترينينيل اسيتات (14.65%)، ميثيل الايجينول (7.73%)، الفا-ترينول (2.48%)، تربنين-4-ول (2.09%)، اليميسين (2.08%) وسابينين (1.8%). كما اعتمد التعرف الكيفي و الكمي للزيت الطيار على معيار المقارنة بسلسلة مرجعية من الألكانات و مطياف الكتلة و مقارنتها بالنتائج الموجودة في المراجع السابقة. هذا وقد اوضح الزيت الطيار فاعلية مؤثرة ضد خلايا الكبد السرطانية بتركيز 1.83 ميكروجرام لكل مليلتر. كما تم تزويد الدراسة باستخدام تحليل التماثل الجزيئي لمكونات الزيت ضد انزيم كاسباس 3 والذي أبان قدرة 32 مركب على التفاعل مع هذا الأنزيم في اماكن تفعيله. علاوة على ذلك، فقد تم دراسة الشكل الظاهري والتركيب المجهرى لكل من أوراق وأعناق وسيقان النبات في صورتها الكاملة والمسحوقة. اظهرت هذه الدراسة وجود خلايا زيتية وألياف في الأوراق والأعناق والسيقان بالإضافة إلى خلايا هلامية في الأوراق والأعناق وخلايا اسكلار انشيمية في الأوراق والسيقان القديمة بالإضافة إلى شعيرات صغيرة على سطح السيقان الصغيرة.